Available online at www.sciencedirect.com
SCIENCE DIRECT®
Lithos 88 (2006) 56–71
LITHOS
www.elsevier.com/locate/lithos

Provenance implications of Th–U–Pb electron microprobe ages from detrital monazite in the Carboniferous Upper Silesia Coal Basin, Poland

Monika Agnieszka Kusiak [a,b,*], Artur Kędzior [a], Mariusz Paszkowski [a], Kazuhiro Suzuki [b], Ignacio González-Álvarez [c], Bolesław Wajsprych [d], Marek Doktor [a]

[a] Institute of Geological Sciences, Polish Academy of Science, Kraków Research Centre, ul. Senacka 1, 31-002 Kraków, Poland
[b] Center for Chronological Research, Nagoya University, Chikusa-ku, Nagoya 464-8602, Japan
[c] Department of Geological Sciences, University of Saskatchewan, 114 Science Place, Saskatoon, SK, Canada, S7N 5E2
[d] Institute of Geological Sciences, Polish Academy of Science, Department of Geology of Sudetes, ul. Podwale 75, 50-449 Wrocław, Poland

Received 4 February 2005; accepted 16 August 2005
Available online 25 October 2005

Abstract

This paper reports the results of CHIME (chemical Th–U–Pb isochron method) dating of detrital monazites from Carboniferous sandstones in the Upper Silesia Coal Basin (USCB). A total of 4739 spots on 863 monazite grains were analyzed from samples of sandstone derived from six stratigraphic units in the sedimentary sequence. Age distributions were identified in detrital monazites from the USCB sequence and correlated with specific dated domains in potential source areas. Most monazites in all samples yielded ca. 300–320 Ma (Variscan) ages; however, eo-Variscan, Caledonian and Cadomian ages were also obtained. The predominant ages are comparable to reported ages of certain tectonostratigraphic domains in the polyorogenic Bohemian Massif (BM), which suggests that various crystalline lithologies in the BM were the dominant sources of USCB sediments.

Keywords: Provenance; Bohemian Massif; Upper Silesia Coal Basin; Geochronology; Electron microprobe dating; Monazite

1. Introduction

The Upper Silesia Coal Basin (USCB) in Poland is part of a complex group of geological units that comprise a foreland basin system associated with the Carboniferous Variscan orogeny. On the basis of petrological studies, Paszkowski et al. (1995) proposed that the crystalline Bohemian Massif (BM) is the main source of sediments filling the USCB. This proposal can be further supported by comparing age estimates from radioisotope-bearing detrital minerals with lithologies in the BM of known age. The present work is the first extensive geochronological study of sedimentary lithologies in the Upper Silesia Coal Basin. The chemical Th–U-total Pb isochron method (CHIME) of Suzuki et al. (1991) is applied to detrital monazites in order to (1) characterize the ages of sediments in the USCB; (2) compare ages in detrital materials to those of rock-forming events in potential provenance areas; and (3) test the hypothesis that the Bohemian Massif is the dominant source of coarse-grained sediments. The aim

* Corresponding author. Institute of Geological Sciences, Polish Academy of Science, Kraków Research Centre, ul. Senacka 1, 31-002 Kraków, Poland.
E-mail address: mkusiak@nendai.nagoya-u.ac.jp (M.A. Kusiak).

0024-4937/$ - see front matter © 2005 Elsevier B.V. All rights reserved.
doi:10.1016/j.lithos.2005.08.004

of this research is to identify age distributions in detrital monazite and correlate them with specific dated domains in potential source areas.

Monazite is a phosphate of Ce, La, and Th, and is commonly present as a detrital mineral in sedimentary rocks. Monazite typically occurs in sediments as equant subhedral to rounded grains and, despite its strong radioactivity, it is much less susceptible to metamictization than similar radioisotope-bearing minerals, such as uraninite, thorianite and thorite. Monazite is widely used in geochronological studies, either by utilizing U–Pb and Sm–Nd isotope systematics (e.g. Parrish and Tirrul, 1989; Noble and Searle, 1995; Hawkins and Bowring, 1999; Vavra and Schaltegger, 1999; Zhu and O'Nions, 1999; Krohe and Wawrzenitz, 2000), or by electron microprobe chemical dating (Suzuki and Adachi, 1994; Montel et al., 1996; Finger and Helmy, 1998). Radiogenic Pb derived from U and Th decay commonly remains in the monazite crystal lattice (Bosch et al., 2002) and, despite a few documented cases of partial Pb loss from grains (e.g. Suzuki et al., 1994), is generally regarded to be resistant to Pb mobilization by diffusion under high-temperature conditions (Cherniak et al., 2004). CHIME geochronology was developed on the basis of precise electron microprobe analysis (Suzuki and Adachi, 1991). This method is well suited for sedimentary rocks, where a large amount of analyses are required to define age populations. Palaeozoic and older monazites are particularly suitable for electron microprobe dating. A CHIME age has geological meaning only if: (1) all Pb is radiogenic and non-radiogenic ("common" lead) is negligible, and (2) the system, in this case the monazite crystal, remained closed after crystallization (e.g. Parrish, 1990). The Pb detection limit of an electron microprobe determines the precision of chemical age results. The lack of detection of Pb isotopes may lead to a false assumption that monazite is generally concordant, i.e. (1) it does not incorporate appreciable amounts of "common" lead during growth, (2) it is resistant to post-crystallization disturbance and (3) it is mostly free from inheritance (Harrison et al., 2002). Comparative studies between isotopically derived and electron microprobe age estimates, however, indicate that the assumption of concordance is generally valid and that "common" Pb contents are typically negligible (e.g. Williams et al., 1999). The high spatial resolution of the microprobe technique (2–5 μm) allows for the study of heterogeneous mineral grains. This study aims to demonstrate the effectiveness of electron microprobe dating for provenance studies of monazite-bearing sediments.

2. Geological setting

The Upper Silesia Coal Basin constitutes a large late Mississippian to Pennsylvanian marine to non-marine sedimentary basin located in southwestern Poland and the northeastern Czech Republic (Fig. 1). The USCB overlies the Moravo–Silesia Zone to the west and the Kraków–Myszków Zone to the north and northeast. To the south, the basin can be traced by subsurface occurrence of coal beds below Miocene deposits and in nappes in the outer Carpathian Mountains.

The USCB is a remnant of the Carboniferous foreland of the Variscan orogen (Gradziński, 1982). The basement consists of Precambrian crystalline rocks of the Cadomian Brno–Upper Silesia Massif, overlain by Devonian–Mississippian platform carbonates. The foredeep succession includes flysch sediments, overlain by a coal-bearing shallow-marine to non-marine molasse. The Pennsylvanian coal-bearing rocks of the USCB concordantly overlie older strata (Kotas, 1972). The stratigraphic thickness of the coal-bearing sequence is estimated at around 8000 m and decreases eastwards (Kotas, 1982). Syn- to post-Carboniferous erosion removed part of the succession in the west (Fig. 1b). Gradziński (1982) described the depocenters of each stratigraphic unit, showing an eastward gradual shift of the maximum subsidence zone, as commonly observed in flexural foredeep basins.

Based on palaeobotanical, palinological and palaeozoological data, the coal-bearing succession is divided into four, informal series (Fig. 2) that are, in ascending order of stratigraphic age: (1) the Paralic Series (PS) of the Pendleian–Arnsbergian; (2) the Upper Silesia Sandstone Series (USSS) of the Kinderscoutian–Yedonian; (3) the Mudstone Series (MS) of the Langsetian–Duckmantian; and (4) the Cracow Sandstone Series (CSS) of the Bolsovian–Westphalian D (Dembowski, 1972a).

The Paralic Series is interpreted as near-shore marine, deltaic, and fluvial in origin (Doktor and Gradziński, 2002). The Štur marine band (XVI) is the lowest member of this series (Namurian A; Kotas, 1995), whereas the base of the overlying USSS is defined at the bottom of coal seam number 510, which represents the onset of on-shore deposition. The PS is characterized by marine, brackish and fresh-water horizons, and is subdivided into the Petrkovice, Hrušov, Jaklovec and Poruba Beds, based on marine and tuffaceous layers (Kotas and Malczyk, 1972a). Each of these units is composed of conglomerates, sandstones, siltstones, claystones and phytogenic facies. Conglomerate clasts include sedimentary rocks, phyllites, quartz–chlorite and quartz–mica schists, microgranites, gneisses and

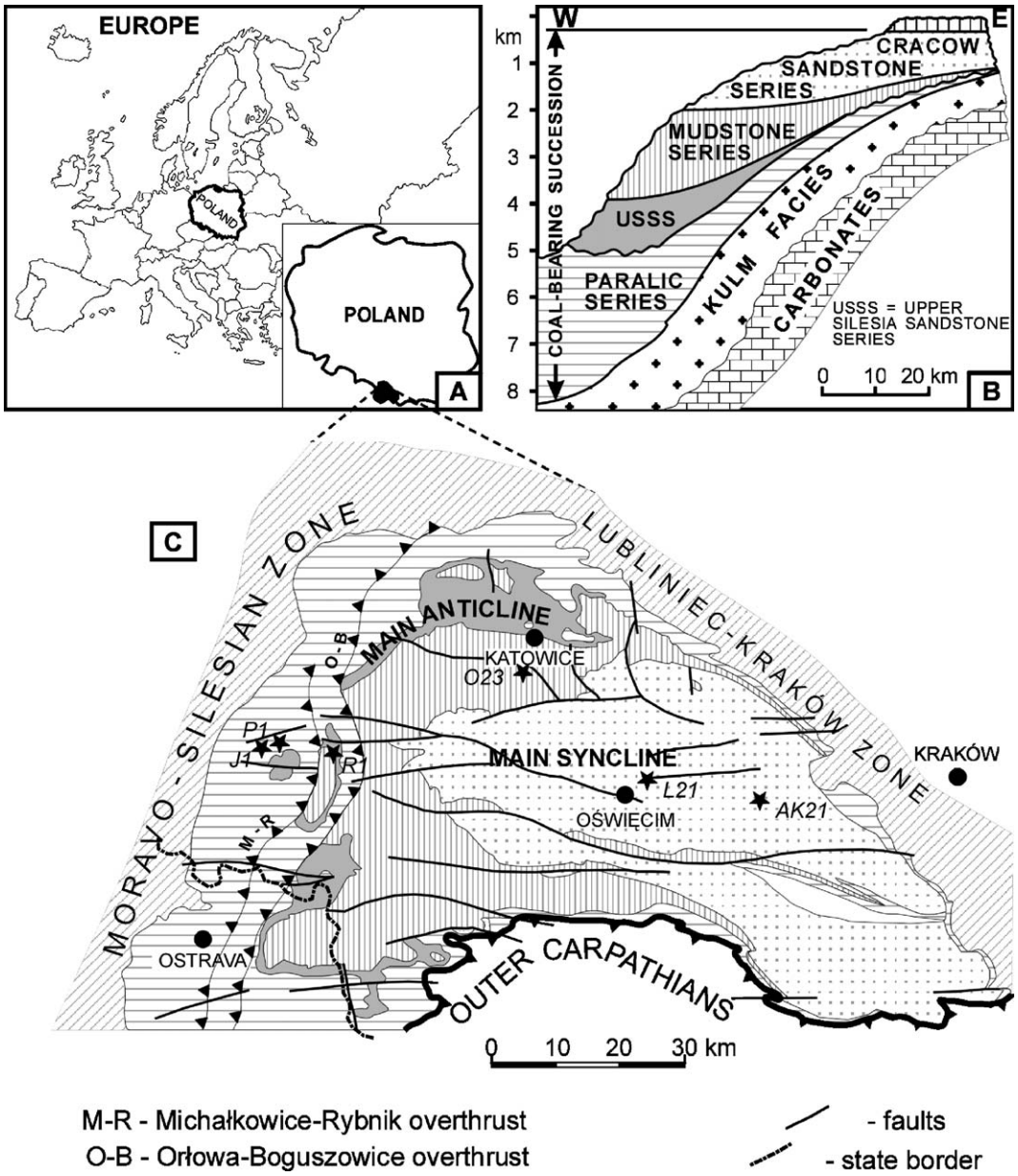

Fig. 1. Generalized geographic location of the Upper Silesia Coal Basin; A — location of USCB, B — main lithostratigraphic units, C — study area and sample location.

granulites (Paszkowski et al., 1995). Sandstones are composed of arkoses, lithic arenites, sublitharenites and subarkoses (Świerczewska, 1995).

The Upper Silesia Sandstone Series is characterized by sandstones and conglomerates deposited in meandering to braided fluvial (Kędzior et al., 2003) and limnic settings (Kotas and Malczyk, 1972b). The series contains subarkoses, sublitharenites and quartz arenites, with lithic clasts of metamorphic rocks, such as quartz–mica and chlorite schists. The USSS has been divided into the Zabrze Beds, overlain by the Ruda Beds, and underlain by the Jejkowice Beds to the west. The Zabrze Beds consist of an approximately 150 m thick sequence of sandstones and conglomerates. The Jejkowice Beds have a similar average petrographic composition to the upper part of the Paralic Series, but have relatively lower amounts of plagioclase (Świerczewska, 1995).

The Mudstone Series is a clastic and phytogenic sequence deposited in an extensive alluvial plain (Doktor and Gradziński, 1985). Based on fresh-water and tufogenic horizons, the MS is subdivided into the Załęże Beds and Orzesze Beds, both dominated by

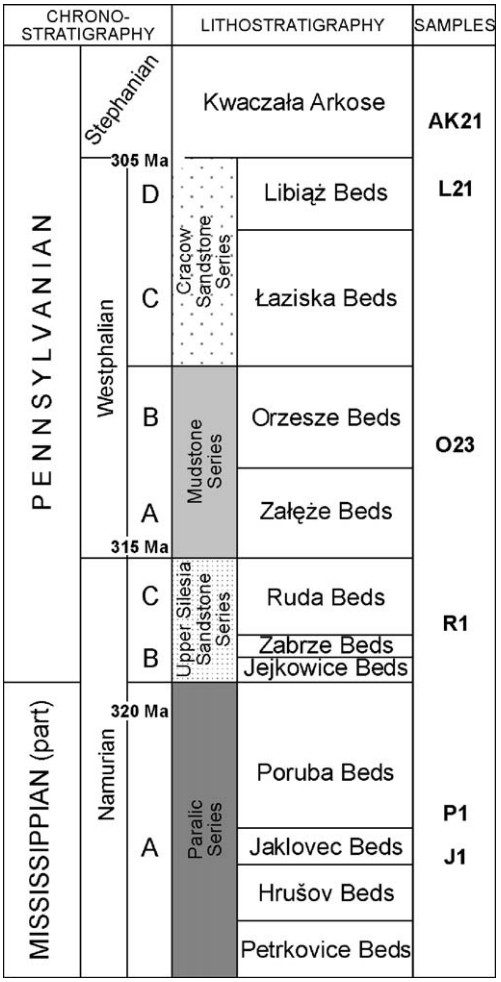

Fig. 2. Simplified stratigraphical scheme of coal-bearing succession of the Upper Silesia Coal Basin.

overbank deposits. Medium-grained sandstones are subarkoses and sublitharenites, in which volcanic grains are prevalent. Świerczewska (1995) suggested that these sediments were derived from felsic acidic rocks.

The Cracow Sandstone Series represents a sharp lithological change from the underlying Mudstone Series. It is subdivided into the Łaziska Beds and the Libiąż Beds, which are separated by a hiatus (Dembowski, 1972b). Both of these units consist of arkoses, lithic arenites, subarkoses and sublitharenitic sandstones, pebbly sandstones and conglomerates, deposited within channels of distal braided rivers (Gradziński et al., 1995). Lithic grains within these facies are dominated by acidic volcanics (Świerczewska, 1995).

The Stephanian Kwaczała Arkose has features of the red-bed facies and contains silicified *Dadoxylons* trunks (Rutkowski, 1972). This unit is broadly similar to the Cracow Sandstone Series (Kotas, 1995), but the Kwaczała Arkose lacks coal seams. As in the CSS, lithic fragments were mostly derived from acidic volcanic rocks (Świerczewska, 1995).

3. Sampling

Samples were collected from underground mines and surface outcrops of each lithostratigraphic unit: (1) two samples from the Paralic Series: J1 from the "Rydułtowy" coal mine and P1 from the Rydułtowy outcrop; (2) one sample from the Upper Silesia Sandstone Series: R1 collected at the "Chwałowice" coal mine in Rybnik; (3) one sample from the Mudstone Series: O23 from the Mikołów brick-factory pit; (4) one sample from the Cracow Sandstone Series: L21 from the "Janina" coal mine; and (5) one sample from the Kwaczała Arkose: AK21, from Gródek Gorge (Figs 1a and 2). Samples were selected to represent the major sedimentary types in the USCB.

Individual rock samples varied between 5 and 20 kg. Samples were crushed and sieved using a 0.32 μm screen. Monazite and other heavy minerals were concentrated from the powders using isodynamic-magnetic and magneto-hydrostatic separators. A description of the heavy mineral separation method is given in Paszkowski et al. (1999). Monazite grains were selected and mounted on glass slides with epoxy, set on a hot plate at 150 °C for 15 min, and polished with diamond paste until most grains were exposed at half-thickness.

4. Analytical method

Monazite was analyzed at the Nagoya University Center for Chronological Research, which houses a JEOL JXA-733 electron microprobe in a temperature-controlled room and optimized solely for EMP chronological research. The JXA-733 is set up with four wavelength-dispersive spectrometers, each with a 140 mm radius Rowland circle, PET diffraction crystal and sealed Xe gas detector, for the simultaneous measurement of ThMα, UMβ, PbMα, and YLα spectral lines. Euxenite provided by Smellie et al. (1978) was used as the standard for Th and U, synthetic glass with 10.18 wt.% PbO for Pb and Pb-free synthetic glass for Y (Suzuki and Adachi, 1998). The instrument was operated at 15 kV accelerating voltage, ~300 nA probe current on the Faraday cup and a beam diameter of 5–7 μm. For the analysis of Th, U, Pb and Y, X-ray intensities were measured in five 80-s cycles on each spectral position (for a total counting time of 400 s). Two optimal background positions, chosen from wavelength-dispersive profiles of a range of typical monazite grains, were measured in five 40-s cycles (total 200 s) above and

below each spectral line position. From these, background values for each line were estimated by interpolation on a linear fit. Background estimations using an exponential fit have been found in some cases to produce lower values (Jercinovic and Williams, 2005; Pyle et al., 2005). In this study, however, wavelength-dispersive profiles examined prior to analysis suggest that the resulting discrepancies in element concentrations (especially for Pb) would be significantly less than the relative errors calculated. Spectral interferences of YLγ and ThMζ on PbMα and ThMγ on UMβ were corrected using the Åmli and Griffin (1975) method.

Raw intensity data from ThMα, UMβ, PbMα, and YLα measurements were converted into concentrations using an analytical data set of natural monazite with a compositional matrix of 0.905 wt.% SiO_2, 11.2 wt.% La_2O_3, 27.4 wt.% Ce_2O_3, 2.68 wt.% Pr_2O_3, 12.0 wt.% Nd_2O_3, 2.12 wt.% Sm_2O_3, 0.705 wt.% Gd_2O_3, 0.16

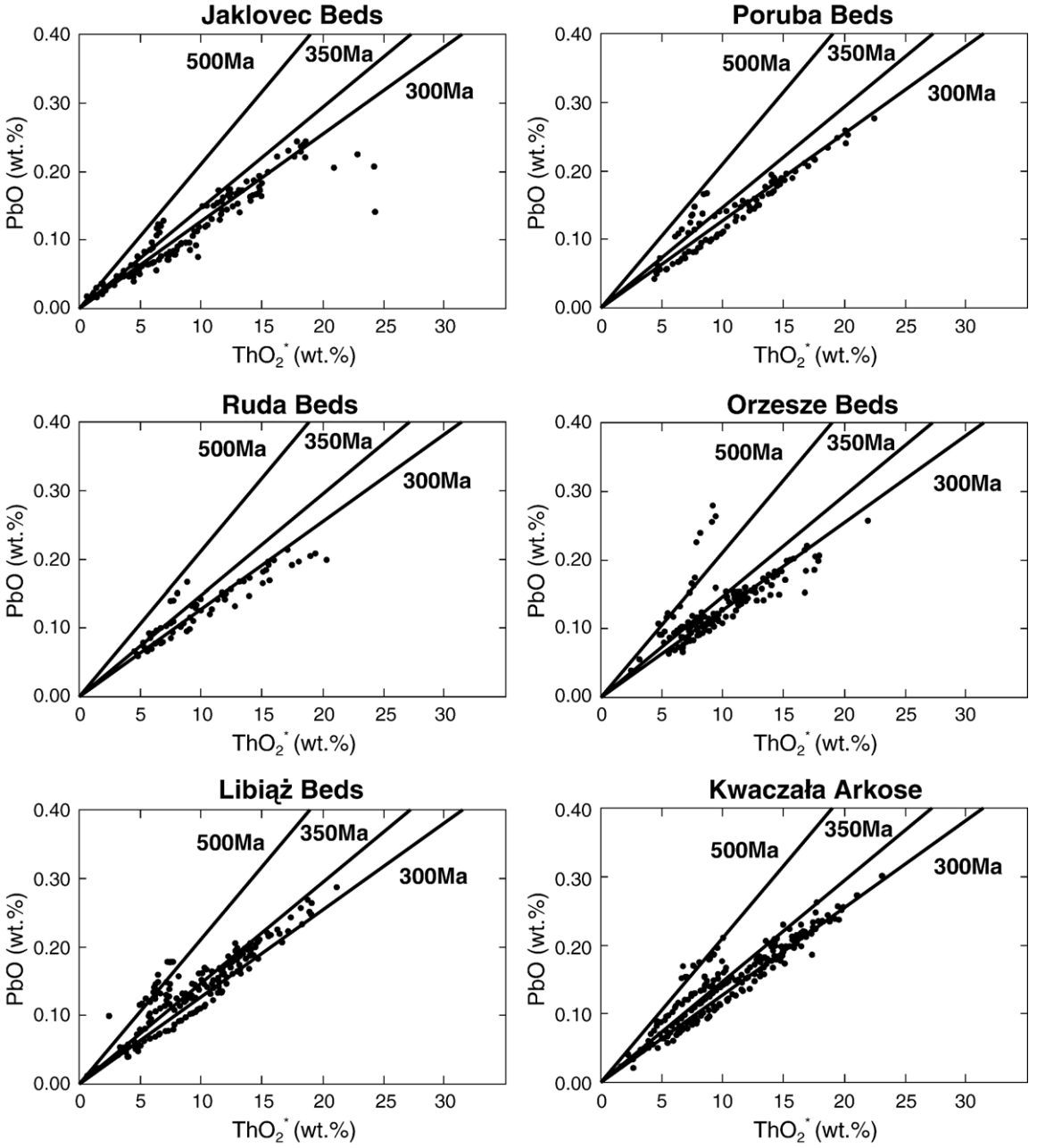

Fig. 3. Plot of PbO vs. ThO_2*, distribution of apparent ages for monazite grains from particular sandstone series of the Upper Silesia Coal Basin.

wt.% Tb_2O_3, 0.21 wt.% Dy_2O_3, 1.29 wt.% CaO and 28.6 wt.% P_2O_5. Small differences in the compositional matrix produce a negligible effect in ThO_2, UO_2, PbO, and Y_2O_3 determinations, and errors are estimated at ≤1% of concentrations, comparable to uncertainties in X-ray counting statistics. Detection limits at a 2σ confidence level are 0.009, 0.012 and 0.006 wt.% for ThO_2, UO_2 and PbO, respectively. The relative errors are about 10% for 0.03 wt.% PbO, 5.0% for 0.1 wt.% UO_2, and 0.5% for 7.0 wt.% ThO_2.

Single-spot analysis ages were calculated using the method described in Suzuki and Adachi (1991) and Suzuki and Adachi (1998). Age errors at 2σ are estimated from counting statistics to be about 20 Ma. Since detrital monazite in sedimentary rocks is not typically derived from a single provenance, isochrons were not calculated for the data.

5. Results

A total of 4739 analyses were carried out by electron microprobe on 863 monazite grains from sandstone samples of the Carboniferous USCB (Fig. 3). Numbers of monazite grains and spots analyzed in each sample are listed in Table 1, along with compositional ranges. Usually five to ten analytical spots were done on each grain to check the homogeneity of the chemical composition and age in the monazite. Table 2 contains 20 representative analyses from each sample. The following supplemental data are available for viewing at the URL listed below.

Analyzed monazite grains vary greatly in shape and size. They are predominantly well rounded and oblate, although euhedral grains are also present and the degree of abrasion on grains is highly variable. Backscattered electron imaging on a scanning electron microscope reveals that most grains are compositionally homogeneous, with fewer grains showing sector zoning, irregular patches and areas of monazite recrystallization or regrowth.

Variations in Th, U and Y contents are much greater between monazite grains from the same sample than within individual grains. Thorium content ranges from 0.29 wt.% ThO_2 for sample J1 to 27.9 wt.% ThO_2 for sample P1, but values higher than 20 wt.% are rare. Uranium content ranges from 0.06 wt.% UO_2 for sample OR23 to 3.03 wt.% UO_2 for sample AK21. Average U contents for each stratigraphic level range from 0.51 to 0.67 wt.% UO_2. Lead content ranges from 0.01 wt.% PbO for sample L21 up to 0.38 wt.% PbO for sample P1, with sample averages varying from 0.08 to 0.13 wt.% PbO. No systematic correlation between thorium content and calculated ages could be identified. Multiple spot analyses on most individual grains have similar ThO_2 and UO_2 contents and ages. Grains with variable ThO_2 contents generally have identical ages within analytical error. Yttrium content averages for each sample range from 3 to 4 wt.% Y_2O_3, and is highest at 7.26 wt.% for a grain from sample L21, which is exceptionally high for monazite. Jonasson et al. (1988) demonstrate that monazites formed in high-temperature mineral assemblages can contain up to 5% Y_2O_3. Monazite with 7 wt.% Y_2O_3 has also been found associated with hydrothermal activity (Schandl and Gorton, 2004). There is a positive correlation between Y and U contents.

Table 1
Monazite sample-set analysis from the USCB Poland

Sample group	J1	P1	R1	O23	L21	AK21
Number of analyses performed	666	1012	172	519	781	1589
Number of grains analyzed	67	203	23	100	152	318
Y_2O_3 average content	1.98	1.41	1.83	2.06	2.24	1.59
Minimum Y_2O_3 value	0.04	0.02	nd	0.10	nd	0.01
Maximum Y_2O_3 value	4.20	3.58	3.59	4.06	7.26	3.97
ThO_2 average content	6.53	8.18	6.63	7.45	6.42	6.80
Minimum ThO_2 value	0.29	0.94	3.41	3.59	0.48	1.15
Maximum ThO_2 value	21.2	27.9	19.2	15.4	18.5	20.4
UO_2 average content	0.59	0.55	0.51	0.67	0.60	0.65
Minimum UO_2 value	0.08	0.08	0.21	0.08	nd	0.06
Maximum UO_2 value	2.42	2.15	1.23	1.71	2.97	3.03
PbO average content	0.11	0.13	0.10	0.12	0.11	0.12
Minimum PbO value	0.02	0.02	0.06	0.06	0.01	0.02
Maximum PbO value	0.24	0.38	0.21	0.22	0.28	0.30
Minimum age [Ma]	139	252	230	215	234	192
Maximum age [Ma]	652	545	444	717	545	546

All analyses are given in wt.%; nd — not detected.

Table 2
Electron microprobe analyses of Y_2O_3, ThO_2, UO_2, PbO, ThO_2* [wt.%] (total ThO_2 and ThO_2 equivalent of measured UO_2) and apparent age [Ma]

Pt#	Y_2O_3	ThO_2	UO_2	PbO	ThO_2*	AGE	Pt#	Y_2O_3	ThO_2	UO_2	PbO	ThO_2*	Age
JMO1-1	1.27	3.96	0.54	0.08	5.72	342	OMO1-1	2.38	5.40	0.61	0.09	7.38	296
JMO1-2	1.28	4.21	0.52	0.09	5.90	344	OMO1-2	2.39	5.42	0.61	0.09	7.40	302
JMO1-3	0.76	3.98	0.53	0.07	5.70	296	OMO1-3	0.36	6.92	0.70	0.11	9.20	271
JMO1-4	1.12	4.54	0.55	0.09	6.33	330	OMO1-4	2.89	5.29	0.78	0.11	7.84	332
JMO1-5	1.17	4.60	0.43	0.08	6.00	318	OMO1-5	1.63	5.88	0.65	0.10	8.00	287
JMO1-6	2.42	4.27	0.52	0.08	5.96	323	OMO1-6	2.04	5.67	0.68	0.11	7.87	316
JMO1-7	2.19	4.12	0.53	0.08	5.86	319	OMO2-1	2.49	6.89	0.66	0.12	9.05	299
JMO1-8	2.48	4.79	0.46	0.10	6.29	359	OMO2-2	2.27	6.83	0.79	0.11	9.40	282
JMO1-9	0.69	7.95	0.55	0.13	9.73	315	OMO2-3	1.61	7.48	0.31	0.10	8.48	287
JMO1-10	2.32	4.65	0.51	0.08	6.30	313	OMO2-4	1.49	8.36	0.29	0.12	9.30	309
JMO2-1	1.41	7.36	0.17	0.09	7.93	274	OMO2-5	1.37	8.24	0.28	0.11	9.14	282
JMO2-2	1.65	8.25	0.19	0.12	8.85	316	OMO2-6	2.16	8.29	0.39	0.12	9.54	297
JMO2-3	1.46	8.10	0.20	0.10	8.74	282	OMO2-7	2.59	7.74	0.85	0.14	10.50	314
JMO2-4	1.53	8.15	0.20	0.11	8.80	301	OMO2-8	1.87	7.69	0.35	0.11	8.81	285
JMO2-5	1.26	7.71	0.16	0.10	8.24	294	OMO3-1	2.67	4.46	0.96	0.11	7.59	325
JMO2-6	1.80	7.76	0.23	0.10	8.51	281	OMO3-2	2.21	5.18	0.90	0.11	8.11	314
JMO2-7	1.16	7.66	0.16	0.10	8.16	294	OMO3-3	2.28	4.65	0.79	0.10	7.22	313
JMO2-8	1.37	7.93	0.18	0.10	8.50	284	OMO3-4	2.67	4.47	0.93	0.10	7.51	303
JMO2-9	1.09	7.62	0.16	0.11	8.14	316	OMO3-5	2.38	4.54	0.83	0.09	7.23	300
JMO2-10	1.20	7.54	0.17	0.10	8.08	289	OMO3-6	2.20	6.86	1.29	0.15	11.10	324
PMO1-1	0.37	9.97	0.19	0.13	10.60	286	LMO1-1	2.57	6.26	0.41	0.10	7.58	307
PMO1-2	0.39	9.85	0.17	0.12	10.40	281	LMO1-2	2.85	6.16	0.43	0.09	7.56	295
PMO1-3	0.37	9.36	0.17	0.12	9.91	283	LMO1-3	2.93	6.04	0.44	0.10	7.45	315
PMO1-4	0.35	9.52	0.17	0.12	10.10	282	LMO1-4	2.84	6.10	0.43	0.10	7.51	319
PMO1-5	0.33	9.36	0.18	0.12	9.95	276	LMO1-5	2.87	6.12	0.43	0.10	7.53	310
PMO2-1	0.91	22.70	1.07	0.33	26.20	297	LMO2-1	1.88	6.35	0.84	0.12	9.10	313
PMO2-2	0.90	22.90	0.74	0.33	25.40	305	LMO2-2	2.01	6.78	1.38	0.15	11.30	312
PMO2-3	0.84	19.10	0.46	0.28	20.60	316	LMO2-3	2.19	5.94	0.80	0.11	8.55	306
PMO2-4	0.82	13.60	0.46	0.19	15.10	298	LMO2-4	0.91	9.26	1.04	0.16	12.60	304
PMO2-5	0.74	13.30	0.45	0.19	14.70	310	LMO2-5	0.95	9.28	0.99	0.16	12.50	309
PMO3-1	0.48	6.26	0.71	0.11	8.57	297	LMO3-1	3.22	6.19	0.70	0.13	8.47	371
PMO3-2	0.36	7.94	0.93	0.14	11.00	301	LMO3-2	0.63	5.53	0.66	0.10	7.69	309
PMO3-3	0.30	12.20	0.97	0.19	15.40	292	LMO3-3	1.51	4.97	0.50	0.08	6.61	298
PMO3-4	0.31	10.90	0.94	0.17	13.90	287	LMO3-4	2.65	4.77	0.46	0.08	6.26	319
PMO3-5	0.26	6.66	0.82	0.12	9.31	303	LMO3-5	2.51	5.36	0.35	0.10	6.49	346
PMO4-1	0.39	5.85	0.75	0.09	8.27	258	LMO4-1	0.13	3.35	0.51	0.06	5.00	272
PMO4-2	0.28	6.92	0.44	0.09	8.33	269	LMO4-2	0.14	4.63	0.71	0.09	6.94	298
PMO4-3	0.29	7.86	1.28	0.14	12.00	276	LMO4-3	0.14	3.30	0.56	0.07	5.11	303
PMO4-4	0.29	6.67	0.72	0.10	9.01	264	LMO4-4	0.14	3.27	0.52	0.06	4.95	299
PMO4-5	0.95	5.86	0.95	0.11	8.94	299	LMO4-5	0.13	3.27	0.52	0.06	4.95	294
RMO1-1	2.61	5.24	0.53	0.09	6.96	308	KMO1-1	2.50	6.14	1.15	0.13	9.89	316
RMO1-2	2.96	4.46	0.85	0.09	7.24	296	KMO1-2	2.52	5.36	1.00	0.11	8.61	304
RMO1-3	2.68	5.05	0.63	0.10	7.10	317	KMO1-3	2.45	5.10	0.83	0.10	7.81	311
RMO1-4	2.93	4.54	0.85	0.09	7.30	296	KMO1-4	2.28	5.02	0.82	0.10	7.68	310
RMO1-5	2.89	5.07	0.72	0.10	7.41	312	KMO1-5	2.17	5.23	0.72	0.11	7.57	338
RMO1-6	2.79	5.25	0.63	0.10	7.29	311	KMO2-1	0.63	4.77	0.16	0.06	5.28	284
RMO1-7	2.36	6.23	0.52	0.10	7.91	311	KMO2-2	0.62	4.89	0.16	0.07	5.42	289
RMO1-8	3.52	5.62	0.44	0.10	7.05	342	KMO2-3	0.60	4.90	0.17	0.07	5.45	294
RMO1-9	3.37	4.97	0.40	0.09	6.28	326	KMO2-4	0.59	4.35	0.14	0.06	4.82	301
RMO1-10	2.63	4.93	0.59	0.09	6.87	308	KMO2-5	0.53	6.18	0.20	0.08	6.82	284
RMO2-1	3.39	5.80	1.14	0.13	9.51	328	KMO3-1	2.04	5.38	0.55	0.10	7.15	324
RMO2-2	3.34	5.73	1.13	0.13	9.42	315	KMO3-2	1.83	5.43	0.48	0.10	7.00	327
RMO2-3	2.93	5.79	1.02	0.13	9.13	335	KMO3-3	1.71	6.21	0.40	0.10	7.51	312
RMO2-4	2.98	5.80	1.02	0.12	9.14	317	KMO3-4	1.71	5.05	0.38	0.08	6.28	316
RMO2-5	3.24	6.09	1.17	0.14	9.91	332	KMO3-5	1.70	5.56	0.39	0.09	6.83	326
RMO2-6	2.95	5.75	1.01	0.13	9.05	326	KMO4-1	2.67	6.32	0.40	0.11	7.63	327

Table 2 (*continued*)

Pt#	Y_2O_3	ThO_2	UO_2	PbO	ThO_2*	AGE	Pt#	Y_2O_3	ThO_2	UO_2	PbO	ThO_2*	Age
RMO2-7	2.92	5.76	1.01	0.13	9.04	333	KMO4-2	2.71	5.63	0.53	0.10	7.36	334
RMO2-8	3.16	5.44	1.05	0.12	8.86	314	KMO4-3	2.73	6.16	0.46	0.10	7.66	319
RMO2-9	3.16	5.49	1.05	0.12	8.92	313	KMO4-4	2.54	5.51	0.60	0.10	7.46	310
RMO2-10	3.16	5.74	1.12	0.13	9.40	328	KMO4-5	2.17	4.55	0.36	0.08	5.73	333

Single-spot age distributions for samples J1, O23, L21, and AK21 are nearly identical (Fig. 4). For all samples analyzed, most single-spot analysis ages fall within the 280–340 Ma range with a strong mode in the 300–320 Ma range. Age distributions in the 280–340 Ma range are skewed towards younger ages in all

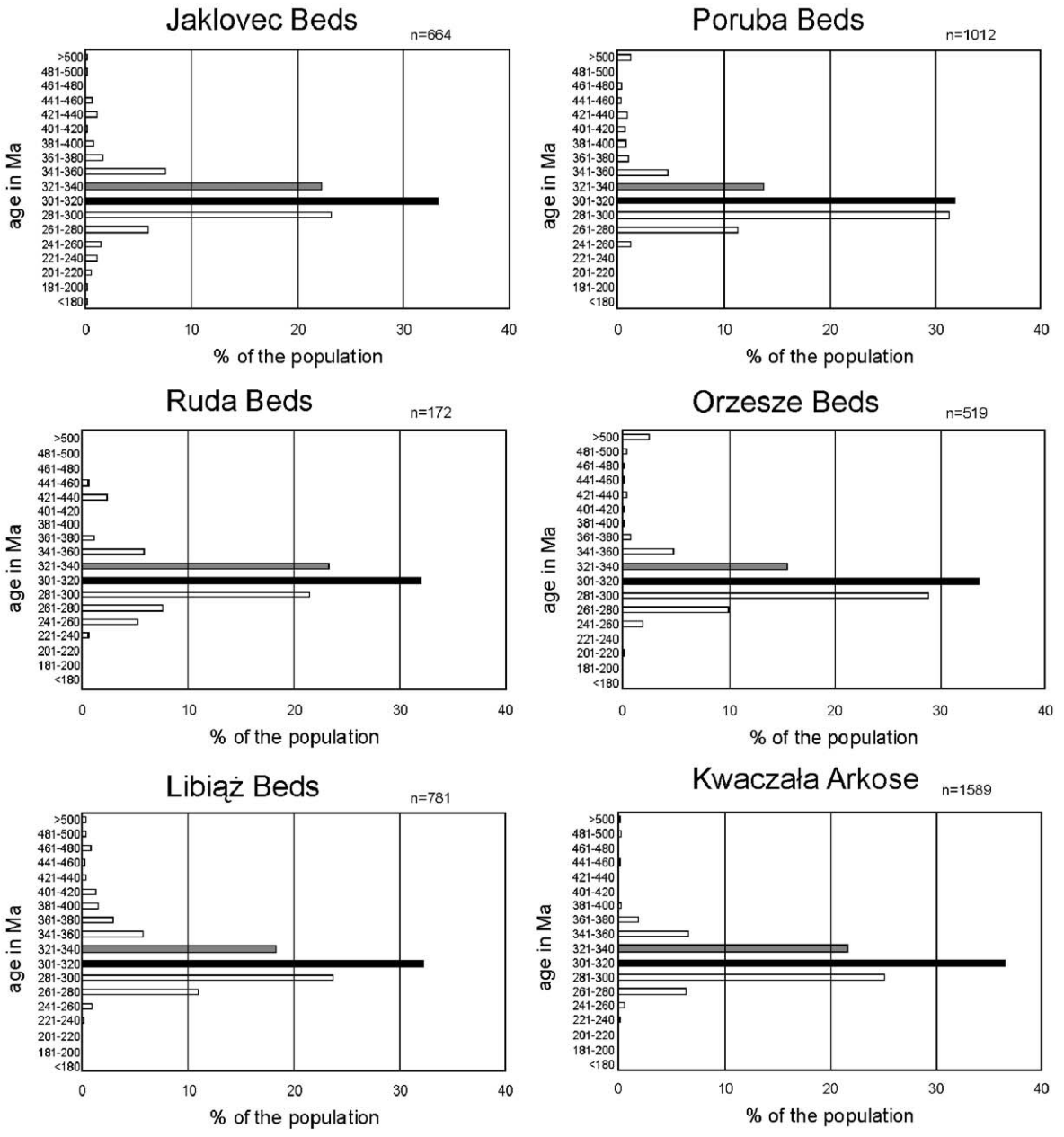

Fig. 4. Histograms of the CHIME age pattern for monazites from particular sandstone series of the Upper Silesia Coal Basin.

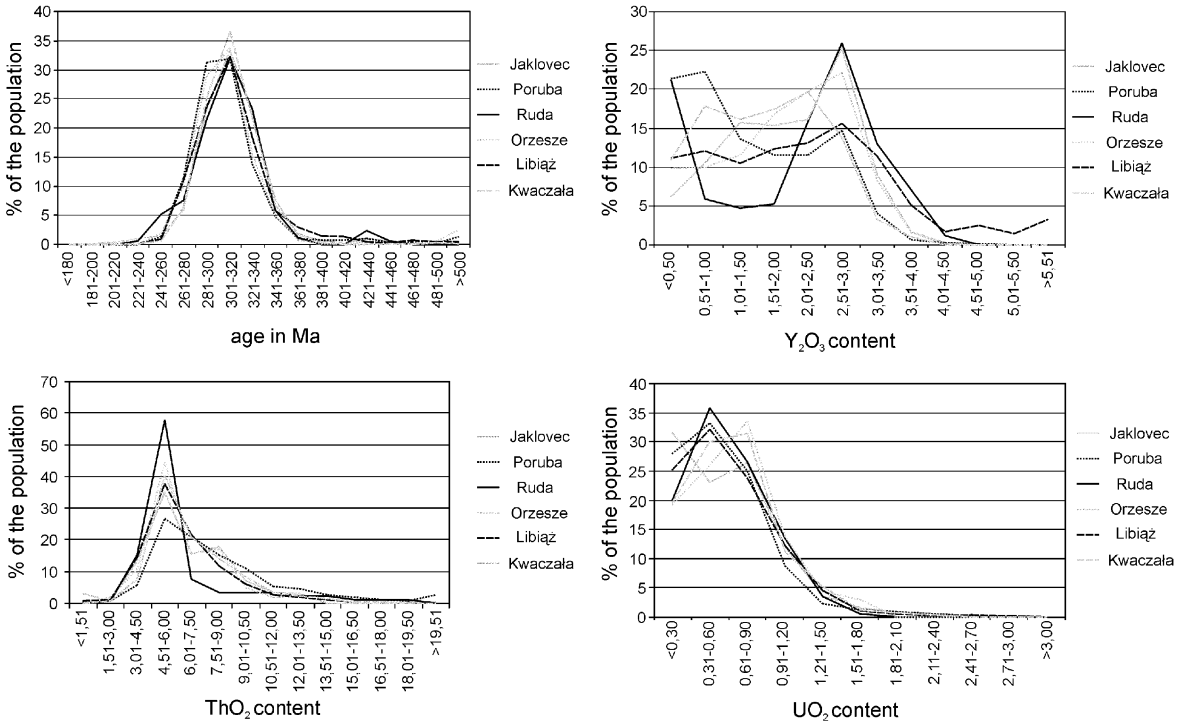

Fig. 5. Distribution of the a) CHIME ages; b)Y_2O_3 content; c) ThO_2 content, d) UO_2 content from the sandstone samples.

samples except R1, where they are skewed towards older ages. All samples have smaller modal distributions in the 420–440 Ma range as well. Ages older than 500 Ma are also present in all samples except R1. Ages obtained from heterogeneous monazite grains do not differ greatly from their homogeneous counterparts. Gaussian curves comparing age clusters with U, Th, and Y content are displayed in Fig. 5. Comparisons of backscattered electron images, analyzed Th, U and Y contents, and single-spot analysis ages of monazite grains revealed no systematic correlations between these variables.

6. Discussion

Based on petrographic and palaeontological evidence from exotic pebbles in the coal-bearing succession, the Bohemian Massif was suggested as the main source area for the USCB sediments (Paszkowski et al., 1995 and references therein). To correlate potential source terranes with detrital materials, published research was reviewed in order to identify (1) monazite-bearing lithologies within the BM that resemble crystalline clasts in the USCB; and (2) age distributions in the BM corresponding to those obtained in this study from the sedimentary succession.

6.1. Monazite-bearing rocks of the Bohemian Massif

Kodymová and Kodym (1984) sampled a wide variety of magmatic, metamorphic and sedimentary rocks at 332 randomly distributed sites in the Bohemian Massif, to characterize the occurrence of heavy minerals. The average monazite contents in crystalline rocks of the BM vary from trace amounts in pyroxene granulite, up to 6.7% of the heavy mineral fraction in the granitoids of the Moldanubian Pluton (equivalent to 176 g/t of bulk rock). Monazite is present in sparse amounts in Palaeozoic sediments of the BM, except for Permo–Carboniferous sandstones in intramontane basins, especially the Plzeň Basin (Fig. 6), where monazite contents amount to 4.6% of the heavy mineral fraction.

Detrital monazite can be derived either directly from the erosion of lithologies in which the mineral was grown, or from the erosion of pre-existing sedimentary deposits. Despite having a hardness of only 5, monazite can be readily recycled from weakly cemented siliciclastic sediments. There are only a few basin-fills in the BM area which could potentially deliver recycled detrital monazite to the USCB. These are (1) Devonian sediments in the Hradec Kralove Basin in the Teplá-Barrandian terrane; (2) Devonian sediments of the

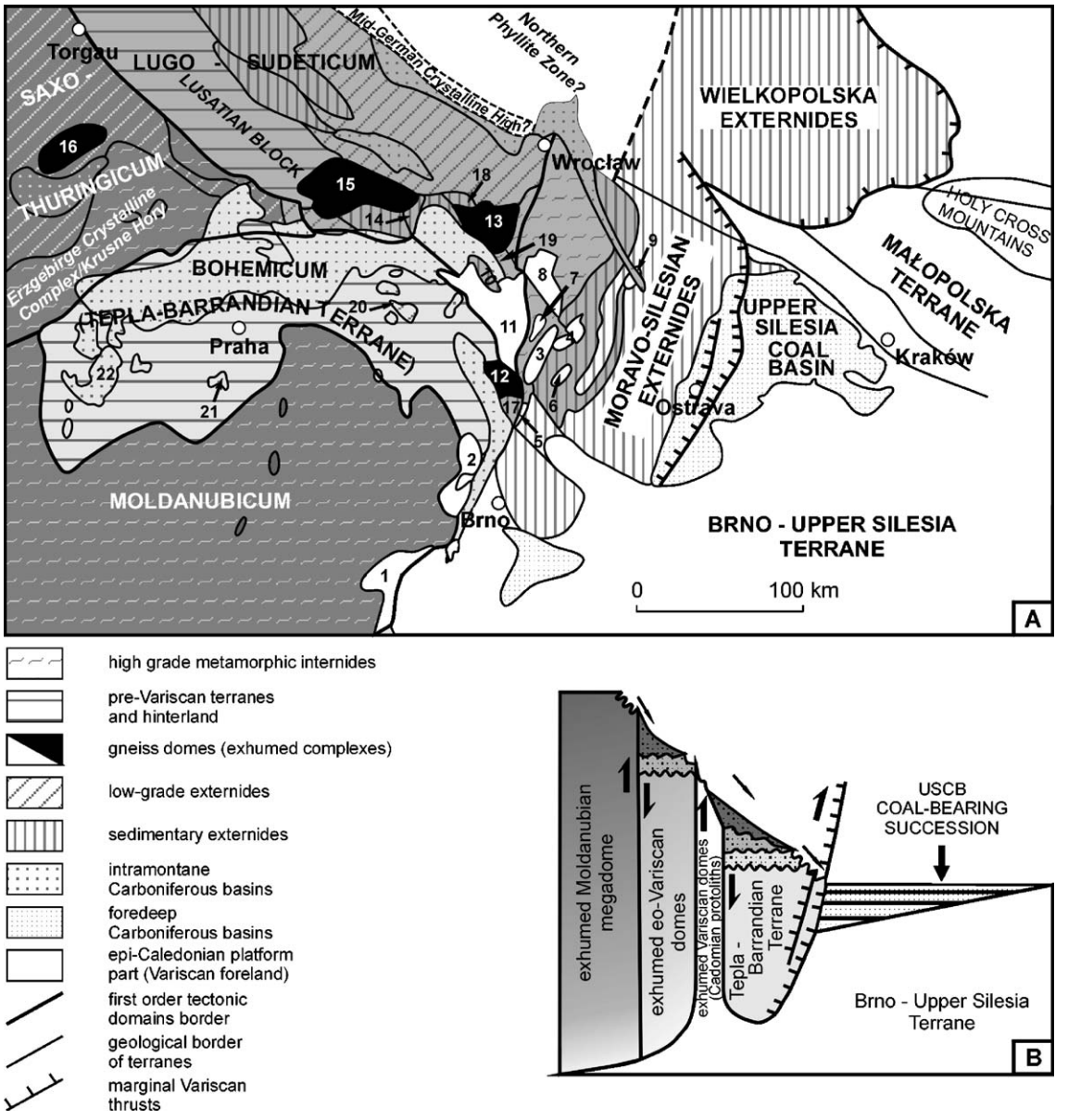

Fig. 6. A) Structural mosaic of Variscan Bohemian Massif and their foreland showing space distribution and tectonostratigraphic affinity of constituent metamorphic core complexes (crystalline domes). Important notice: Zabreh crystalline complex (Zabreh dome) is not a part of Variscan Moldanubicum composite megadome. Particular exhumed units: Cadomian/Variscan: 1. Thaya (Dyje) dome, 2. Svratka dome, 3. Keprnik dome, 4. Desna dome, 5. Rohle dome, 6. Oskava dome, 7. Velké Vrbno dome, 8. Vidnava dome, 9. Biała dome, 10. Kłodzko dome (structurally upper subunits of exhumed Kłodzko Metamorphic Unit). Caledonian?/Variscan: 11. Orlica–Śnieżnik dome. Eo-Variscan: 11. Kłodzko dome (structurally lower subunits of exhumed Kłodzko Metamorphic Unit), 12. Zabreh dome, 13. Góry Sowie dome, 14. Rychory Mts., 15. Karkonosze dome, 16. Granulite Mts. dome (Granulitgebirge). Eo-Variscan syn-exhumational basins: 17. Mohelnice Unit, 18. Świebodzice Depression, 19. Bardo Mountains parautochthonous Unit, 20. Hradec Kralove Basin, 21. Rozmitál Islet, 22. Plzeň Basin. B) General tectonostratigraphic model of telescoping, successive exhumations in Bohemian Massif polyorogenic crystalline dome system as syn-sedimentary active source terrains for siliciclastics of the Upper Silesia foreland basin.

Bardo Mountains autochthon, which unconformably overlie the Kłodzko Metamorphic rocks; and 3) Upper Devonian conglomerates and sandstones of the Świebodzice Basin (Fig. 6A; Porębski, 1981, 1990). However, the major source of recycled detrital monazite is likely to be the weakly cemented and monazite-rich sandstones of the Carboniferous intramontane basin system (Fig. 6B), which forms a ‘cascade’ of sedimen-

tary catchments between the BM and the USCB. Due to the isolation of monazite grains in the USCB sediments, however, the proportion of recycled detrital monazite to that derived by direct erosion is very difficult to determine. Lithic clasts with sedimentary origins were examined but provided no correlations of source with detrital monazite in equivalent units of the USCB. For example, in the Libiąż Beds and Kwaczała Arkose, up to 30% of clasts consist of greywacke, which was probably derived from a thick Upper Proterozoic siliciclastic-volcanic sequence of units in the Teplá-Barrandian terrane. The detrital provenance of this sequence, however, is of a shallowly dissected volcanic arc, which is unlikely to be a significant source of monazite.

6.2. Monazite age distributions in the USCB and BM

The sedimentary architecture of the USCB sequence has two important characteristics. Firstly, there are sharp transitions in the sedimentary column, both in the average thickness and abundance of coarse-grained lithosomes and in the grain sizes of sediments. These transitions are attributed to rapid changes in the supply rate and fraction of fluvial sediments. The clearest example is the sudden appearance of thick, coarse-grained lithosomes at the contact between Mudstone Series and Cracow Sandstone Series. Secondly, there are large changes in depositional systems between stratigraphic units, as observed in the transition between the Paralic Series and the Upper Silesia Sandstone Series (Gradziński et al., 2004). Despite these changes, which strongly affect the entire basin, the age distribution pattern of detrital monazite in the USCB lithologies reveals no distinct differences between the sandstone units sampled.

Most monazite grains in all samples analyzed yielded 300–320 Ma ages, which correspond to the timing of the Variscan orogeny. Pre-Variscan ages were also obtained, including ages corresponding to the timing of the Cadomian and Caledonian orogenies. All three orogenic episodes produced lithologies in the Bohemian Massif. More problematic are the occurrence of late to post-Variscan monazite ages, which are younger than the previously determined stratigraphic ages of the sandstone series. In order to compare monazite age distributions with the ages of tectonostratigraphic domains in the polyorogenic BM, age data with continuous distributions between 340 and 280 Ma were binned in 20 Ma intervals.

On exposed surfaces of the BM, a complex mosaic of crystalline domains can be observed, each characterized by distinct protolith, metamorphic and post-peak metamorphic cooling ages. The mosaic represents a polyorogenic set of exhumed crystalline bodies, including metamorphic core-complexes and associated plutons. These bodies can be grouped by time of formation into Cadomian, Caledonian, eo-Variscan and Variscan ages (see Fig. 6B).

6.2.1. Variscan sources for detrital monazite in the Bohemian Massif

The modal age range for all samples analyzed from the USCB (300–320 Ma) corresponds to the Sudetean–Asturian phase of the Variscan orogeny, the final major tectonothermal event that formed the BM. During the final, Sudetian phase of Variscan orogenesis, the partially molten mid to lower crust was overthickened, leading to the rapid uplift and exhumation of metamorphic core complexes and the subsequent collapse of the orogen. This phase is related to the final and most important episode of erosion of highly elevated topography in the BM. Rapid exhumation and post-orogenic collapse are indicated by the almost syn-sedimentary cooling ages of detrital muscovite (K–Ar dating by Banas et al., 1995; Ar–Ar dating by Schneider and Manecki, 2005) and the ages of monazite grains (Kusiak et al., 2001; Lekki et al., 2002) in the USCB sediments. The exhumation rate is estimated at ~10 km for the first 20 m.y. (Zulauf et al., 2002). This rapid uplift would have generated an elevated relief higher than the permanent snow line, subjecting exposed rock to intense physical weathering and producing copious amounts of extremely immature siliciclastic detritus.

The Moldanubian metamorphic complex, together with associated plutons (Gerdes et al., 1998, 2000; Janoušek et al., 2004), is the largest exposed crystalline core complex in the BM (Bues et al., 2002). Franz et al. (1996) distinguished several metamorphic events in the Moldanubian complex. Granulite-grade metamorphism occurred ca. 340 Ma (Kröner et al., 2000). Metamorphism ended with the rapid uplift of the Moldanubian complex shortly after (340 Ma; Friedl et al., 2004). Within the Moldanubian complex, high-grade metamorphism resulted in formation of the syn- to post-tectonic Moldanubian and Central Bohemian Plutons. The Moldanubian Pluton, a group of granitoid intrusions that include the South Bohemian Batholith, was emplaced around 300–330 Ma from magma generated by the partial melting of pre-existing Cadomian crust (Gerdes et al., 2000). Most Moldanubian crystalline rocks are relatively rich in monazite, and the South Bohemian Pluton contains the highest concentration of monazite among BM lithologies (Kodymová and Kodym, 1984).

Erosion of the Moldanubian complex and associated plutons during the Variscan age would have provided an excellent source for detrital monazite in the intramontane basins of the BM and in the foreland USCB. There is some debate, however, as to whether the plutons would have been exposed to erosion during the Variscan orogeny. Petránek (1978) considered the granitoids to have been completely covered by metamorphic country rocks throughout the Late Carboniferous. Other studies indicate that the plutons were exposed at this time (Kukal, 1984; Vlašimský, 1986). The age correlation between most of the detrital monazite in the USCB and 300–340 Ma monazite-rich lithologies associated with the Moldanubian complex supports the latter view.

The Moldanubian complex is polymetamorphic and contains mineral associations with ages that reflect Cadomian and Ordovician tectonothermal events (Friedl et al., 2004; Schenck and Todt, 1981; Van Breemen et al., 1982). If the Moldanubian lithologies are the main source for detritus in the USCB, older age groups from detrital monazite in the USCB samples may represent inherited ages from pre-Variscan events. However, a lack of eo-Variscan ages in the crystalline Moldanubian rocks suggests that they were not affected by tectonothermal activity at this time. This leads us to conclude that they are not the source for eo-Variscan monazite ages from the USCB sandstones.

Several crystalline complexes that were exhumed in the late stages of the Variscan orogeny are distributed along the N-trending Moravo–Silesian Zone, at the eastern edge of Bohemian Massif. These include a series of gneissic domes (from south to north): the Thaya window (a half-dome), the Svratka dome, the Keprnik dome, the Desná dome, the Velké Vrbno dome and the Orlica–Śnieżnik dome (Fig. 6). All of these domes contain ages indicating Variscan metamorphic events overprinting Cadomian protoliths. During the Carboniferous, these deeply buried metamorphic core complexes rose and pierced through an accretionary prism that was derived from the erosion of the Brno–Upper Silesia terrane. U–Pb SHRIMP zircon ages (Turniak et al., 2000) from the Orlica–Śnieżnik dome cluster around the Cadomian (530–540 Ma) and Variscan (ca. 342 Ma) events. However, Borkowska and Dörr (1998) has proposed a younger, Ordovician protolith for the Śnieżnik orthogneisses.

Pre-Variscan age groups from the USCB sandstones can be also attributed to less extensive Cadomian and eo-Variscan crystalline core-complexes in the BM, which were also overprinted by Variscan metamorphism.

6.2.2. Eo-Variscan sources

Eo-Variscan (380–400 Ma) ages from USCB monazite can be correlated with a distinct age population from accessory minerals in exhumed crystalline rocks of the Zabreh metamorphic complex and the Sowie Góry block. Although some authors have grouped the Zabreh complex with the Moldanubian complex, we consider it to have formed during an eo-Variscan high-pressure tectonothermal event. Eo-Variscan ages are also found in the detritus of intramontane sedimentary basins, such as the Świebodzice depression and the Palaeozoic Mohelnice basin.

6.2.3. Caledonian sources

Significant distributions of Caledonian (420–440 Ma) ages were obtained from detrital monazite in all of the USCB samples, except for the Kwaczała Arkose. Such ages are rare in the BM, being found only as protolith ages in rocks from the Izera–Karkonosze and Śnieżnik–Orlica domes (Fig. 6). In Germany, the Variscan Mid-German Crystalline High and the Northern Phyllite Zone both contain relicts of Caledonian protoliths in some orthogneisses, which may represent traces of a hidden, Silurian magmatic arc (comp. Franke and Żelaźniewicz, 2000; Kozłowski et al., 2004). No evidence of Caledonian protoliths, however, has been found in the Fore Sudetic Monocline, which is the eastern extension of the Northern Phyllite Zone. Caledonian ages have been reported in the Góry Sowie block (Cymerman, 1998). However, Franke and Żelaźniewicz (2002) consider these ages to be analytical artifacts. A suitable source, therefore, for Caledonian ages in the USCB has not been yet identified.

6.2.4. Ordovician (eo-Caledonian) sources

Crystalline metamorphic complexes in the BM contain Ordovician magmatic protolith ages (ca. 450–480 Ma), which have been attributed to rifting and the opening of the Rheic Ocean (Crowley et al., 2000). Detrital monazite from the USCB samples, however, did not yield any significant populations of this age. This may indicate that rocks did not deliver detritus to the USCB. It is probable, however, that the age gap is simply due to the scarcity in the BM of Ordovician ages in the rocks exposed by Variscan exhumation.

6.2.5. Cadomian sources

Cadomian crystalline complexes in the BM, weakly overprinted by later metamorphism, provide potential sources for Cambrian and Precambrian detrital ages (Fig. 6). These include 1) the Lusatian Block (LB), a Neoproterozoic complex containing a thick sequence of

greywackes intruded by eo-Cambrian granitoids (Kryza, 2004); 2) the upper sub-units of the Kłodzko Metamorphics (or Kłodzko dome), which yield zircon ages of 590–600 Ma (Mazur et al., 2004); and 3) the Teplá-Barrandian (TB) unit, which is similar in composition and timing to the LB (Drost et al., 2004). The TB unit and the LB are distinguished by the presence in the form of extensive extruded lava flows, whereas only isolated layers of volcanic ash have been noted in the LB. Neoproterozoic sequences in both are intruded by ca. 540 Ma granitoids (Zulauf et al., 1999; Drost et al., 2004).

6.2.6. Ages younger than 300 Ma

Aside from the age ranges discussed above, a significant distribution of ages in the 280–300 Ma range was obtained from all of the USCB samples. These ages are younger than the stratigraphic ages determined for the sandstone series. Due to the relative large errors estimated for calculated ages ($2\sigma = 20$ Ma), most of these ages may not be statistically resolvable from the 300–320 Ma modal distribution. However, they should still be accounted for, and in lieu of petrographic constraints and textural or compositional evidence of multiple stages of growth within detrital monazite grains, several possibilities are suggested. 1) Problems in the analytical method, especially in the estimation of Pb contents, have produced a systematic lowering of age estimates. In particular, overestimation of background values on PbMα by linear interpolation, as described in the Analytical methods section, would lower age estimates. Although estimation of background on PbMα with an exponential model (Jercinovic and Williams, 2005) may produce lower background estimates (Pyle et al., 2005), careful examination by the authors of wavelength-dispersive profiles for typical monazite compositions indicate that the difference is significantly less than 20 Ma on ca. 300 Ma age estimates. 2) The ages resulted from the preferential loss of Pb from monazite and do not represent true ages of monazite growth. This may have been caused by post-sedimentary processes, such as chemical leaching or corrosion by hot fluids percolating through the sandstones during diagenesis. Grains chosen for analysis, however, were generally clear and free from inclusions or evidence of alteration. The sandstone samples lack petrological evidence for the effects of such fluid activity as well. It is also unclear why such processes would preferentially affect Pb. Selective loss of Pb may also have occurred while monazite was still in the source rocks. Such behavior, however, has not been reported yet from crystalline lithologies in the Bohemian Massif. 3) New monazite grew during diagenesis in the USCB sandstones. Weathering and leaching of Th, U and REEs from allanite and monazite, and leaching of phosphorous from apatite, monazite and other minerals can provide a source for the crystallization of monazite from percolating fluids. The high actinide content of crystalline source rocks in the BM, as well as the occurrence of Uranium ore deposits in the Carboniferous sediments of the intramontane Lower Silesia Coal Basin, demonstrate the availability of components for monazite deposition. Although no textural or compositional evidence of such processes were observed in analyzed monazite grains, this possibility is worthy of further investigation. 4) Loss of radon, of which the ^{222}Rn, ^{220}Rn and ^{219}Rn isotopes are intermediate products in the Th and U radioactive decay series, from monazite in liquid was investigated by Garver and Baskaran (2004). Although such loss could be significant adjacent to surfaces, inclusions, cracks and pores, the distance of transport in a crystalline lattice by fission recoil is on a scale of only tens of nanometers. Considering recoil distances and the number of intermediate isotopes that decay by α-particle emission, it is very unlikely that daughter isotopes of Th and U decay would be lost on a scale greater than 1 μm. All of these explanations are presented as working hypotheses. Further work is required to evaluate the relative importance of these suggestions.

7. Conclusions

This study shows the effectiveness of electron microprobe dating for provenance studies of monazite-bearing sediments. The majority of electron microprobe ages obtained in this study of Carboniferous foreland USCB sandstones fall within the 300–340 Ma range, along with subordinate Cadomian, Caledonian and eo-Variscan ages. The detrital monazite ages are comparable to reported ages of tectonostratigraphic domains in the polyorogenic Bohemian Massif, which suggests that various crystalline lithologies in the BM were the dominant sources of USCB sediments. A viable source for monazite with Caledonian ages may be identified by future studies.

Acknowledgements

We express our thanks to S.J. Porębski for his fruitful comments on this study. N. Bakun-Czubarow, R. Gradziński, A. Peterhänsel and E. Turnau are thanked for their thoughtful reviews of earlier drafts of our manuscript. The manuscript has been significantly improved by critical reviews of R. Kryza, J.M. Montel and

J. Pyle. D. Dunkley is thanked for discussions and for improving the language. This research was financially supported by the Polish State Committee for Scientific Research, grant 3PO4D04724, and the Japan Society for the Promotion of Science.

Appendix A. Supplementary data

Supplementary data associated with this article can be found, in the online version, at doi:10.1016/j.lithos.2005.08.004.

References

Åmli, R., Griffin, W.L., 1975. Microprobe analyses of REE minerals using empirical correction factors. Am. Mineral. 60, 599–606.

Banas, M., Paszkowski, M., Clauer, N., 1995. K–Ar ages of white micas from the Upper Carboniferous rocks of Upper Silesia Coal Basin. Stud. Geol. Pol. 108, 21–25.

Borkowska, M., Dörr, W., 1998. Some remarks on the age and mineral chemistry of orthogneisses from the Lądek–Śnieżnik Metamorphic Massif–Sudetes, Poland. Terra Nostra 98, 27–30.

Bosch, D., Hammor, D., Bruguier, O., Caby, R., Luck, J.M., 2002. Monazite "in situ" $^{207}Pb/^{206}Pb$ geochronology using a small geometry high-resolution ion probe: application to Archaean and Proterozoic rocks. Chem. Geol. 184, 151–165.

Bues, C., Dörr, W., Fiala, J., Vejnar, Z., Zulauf, G., 2002. Emplacement depths and radiometric ages of Paleozoic plutons of the Neukirchen–Kdyně Massif: differential uplift and exhumation of Cadomian basement due to Carboniferous orogenic collapse (Bohemian Massif). Tectonophysics 352, 225–243.

Cherniak, D.J., Watson, E.B., Grove, M., Harrison, T.M., 2004. Pb diffusion in monazite: a combined RBS/SIMS study. Geochim. Cosmochim. Acta 68, 829–840.

Crowley, Q.G., Floyd, P.A., Winchester, J.A., Franke, W., Holland, J.G., 2000. Early Palaeozoic rift-related magmatism in Variscan Europe: fragmentation of the Armorican Terrane Assemblage. Terra Nova 12, 171.

Cymerman, Z., 1998. The Góry Sowie terrane: a key to understanding the Palaeozoic evolution of the Sudetes area and beyond. Geol. Q. 42 (4), 379–400.

Dembowski, Z., 1972a. Ogólne dane o Górnośląskim Zagłębiu Węglowym. Prace IG 61, 9–22 (in Polish, with English Abstr).

Dembowski, Z., 1972b. Krakowska seria piaskowcowa Górnośląskiego Zagłębia Węglowego. Prace IG 61, 509–537 (in Polish, with English Abstr).

Doktor, M., Gradziński, R., 1985. Środowisko depozycji aluwialnych utworów weglonośnych serii mułowcowej (górny karbon Zagłębia Górnośląskiego). Stud. Geol. Pol. 82, 5–67 (in Polish, with English Abstr.)

Doktor, M., Gradziński, R., 2002. Sedymentacja osadów węglonośnej sukcesji Górnośląskiego Zagłębia Węglowego. Doc. Geonica, 35–40 (in Polish, with English Abstr.)

Drost, K., Linnemann, U., McNaughton, N., Fatka, O., Kraft, P., Gehmlich, M., Tonk, C., Marek, J., 2004. New data of the Neoproterozoic–Cambrian geotectonic setting of the Teplá-Barrandian volcano-sedimentary successions: geochemistry, U–Pb zircon ages, and provenance (Bohemian Massif, Czech Republic). Int. J. Earth Sci. (Geol. Rundsch.) 93, 742–757.

Finger, F., Helmy, H.M., 1998. Composition and total-Pb model ages of monazite from high-grade paragneisses in the Abu Swayel area, southern Eastern Desert, Egypt. Miner. Petrol. 62, 269–289.

Franke, W., Żelaźniewicz, A., 2000. The eastern termination of the Variscides: terrane correlation and kinematic evolution. In: Franke, W., Haak, V., Oncken, O., Tanner, D. (Eds.), Quantification and Modelling in the Variscan Belt. Geol. Soc., London, Special Publ., vol. 179, pp. 63–86.

Franke, W., Żelaźniewicz, A., 2002. Structure and evolution of the Bohemian Arc. In: Winchester, J.A., Pharaoh, T.C., Verniers, J. (Eds.), Palaeozoic Amalgamation of Central Europe. Spec. Publ.-Geol. Soc. London, vol. 201, pp. 279–293.

Franz, G., Andrehs, G., Rhede, D., 1996. Crystal chemistry of monazite and xenotime from Saxothuringian– Moldanubian metapelites, NE Bavaria, Germany. Eur. J. Mineral. 8, 1097–1118.

Friedl, G., Finger, F., Paquette, J.-L., von Quadt, A., McNaughton, N.J., Fletcher, I.R., 2004. Pre-Variscan geological events in the Austrian part of the Bohemian Massif deduced from U–Pb zircon ages. Int. J. Earth Sci. (Geol. Rundsch.) 93, 802–823.

Garver, E., Baskaran, M., 2004. Effects of heating on the emanation rates of radon-222 from a suite of natural minerals. Applied Radiat. Isotopes 61, 1477–1485.

Gerdes, A., Wörner, G., Finger, F., 1998. Late-orogenic magmatism in the southern Bohemian Massif — geochemical and isotopic constraints on possible sources and magma evolution. Acta Univ. Carol., Geol. 42 (2), 41–45.

Gerdes, A., Henk, A., Wörner, G., 2000. Post-collisional granite generation and HT/LP metamorphism by radiogenic heating: the Variscan South Bohemian Batholith. J. Geol. Soc., Lond. 157, 577–587.

Gradziński, R., 1982. Explanatory notes to the lithotectonic molasse profile of the Upper Silesia Basin (Upper Carboniferous–Lower Permian). Veröff. Zentralinst. Phys. Erde. Ad W DDR, Potsdam, pp. 135–225.

Gradziński, R., Doktor, M., Słomka, T., 1995. Depositional environments of the coal-bearing Cracow Sandstone Series (Upper Westphalian), Upper Silesia, Poland. Stud. Geol. Pol. 108, 149–170.

Gradziński, R., Doktor, M., Kędzior, A., 2004. Środowiska i systemy depozycyjne osadów górnokarbońskiej sukcesji węglonośnej Górnośląskiego Zagłębia Węglowego. Polska Konferencja Sedymentologiczna, VII Krajowe Spotkanie Sedymentologów, Materiały Konferencyjne, Zakopane, p. 89. (In Polish).

Harrison, T.M., Catlos, E.J., Montel, J.M., 2002. U–Th–Pb dating of phosphate minerals. In: Kohn, M.J., Rakovan, J., Hughes, J.M. (Eds.), Phosphates: Geochemical, Geobiological, and Materials Importance. Rev. Miner. Geoch., vol. 48, pp. 523–558.

Hawkins, D.P., Bowring, S.A., 1999. U–Pb monazite, xenotime and titanite geochronological constraints on the prograde to post-peak metamorphic thermal history of paleoproterozoic migmatites from the Gran Canyon, Arizona. Contrib. Mineral. Petrol. 134, 150–169.

Janoušek, V., Braithwaite, C.J.R., Bowes, D.R., Gerdes, A., 2004. Magma-mixing in the genesis of Hercynian calc-alkaline granitoids: an integrated petrographic and geochemical study of the Sázava intrusion, Central Bohemian Pluton, Czech Republic. Lithos 78, 67–99.

Jercinovic, M.J., Williams, M.L., 2005. Analytical perils (and progress) in electron microprobe trace element analysis applied to geochronology: background acquisition, interferences, and beam irradiation effects. Am. Mineral. 90, 526–546.

Jonasson, R.G., Bancroft, G.M., Boatner, L.A., 1988. Surface reactions of synthetic, end-member analogues of monazite, xenotime

and rhabdophane, and evolution of natural waters. Geochim. Cosmochim. Acta 52, 767–770.

Kędzior, A., Doktor, M., Martinec, P., 2003. Warunki sedymentacji i architektura ciał piaszczystych warstw zabrskich (namur B) w czeskiej części Górnośląskiego Zagłębia Węglowego - porównanie z częścią polską. XXVI Sympozjum Geologia Formacji Węglonośnych Polski, Kraków, pp. 51–54. (In Polish, with English Abstr.)

Kodymová, A., Kodym, O., 1984. Contents of selected minerals in rocks of the earlier formations of the Bohemian Massif. Èas. Mineral. Geol. 29 (2), 129–140.

Kotas, A., 1972. Osady morskie karbonu górnego i ich przejście w utwory produktywne Górnośląskiego Zagłębia Węglowego. Prace IG 61, 279–328 (in Polish, with English Abstr).

Kotas, A., 1982. Zarys budowy geologicznej Górnośląskiego Zagłębia Węglowego. Przewodnik LIV Zjazdu PTG, pp. 45–72. (in Polish).

Kotas, A., 1995. Lithostratigraphy and sedimentologic-paleogeographic development. Upper Silesia Coal Basin. In: Zdanowski, A., Żakowa, H. (Eds.), The Carboniferous System in Poland, Prace PIG, vol. 168, pp. 124–134.

Kotas, A., Malczyk, W., 1972a. Seria paraliczna piętra namuru dolnego Górnośląskiego Zagłębia Węglowego. Prace IG 61, 329–425 (in Polish, with English Abstr.)

Kotas, A., Malczyk, W., 1972b. Górnośląska seria piaskowcowa piętra namuru górnego Górnośląskiego Zagłębia Węglowego. Prace IG 61, 427–466 (in Polish, with English Abstr.)

Kozłowski, W., Domańska, J., Nawrocki, J., Pécskay, Z., 2004. The provenance of the Upper Silurian greywackes from the Holy Cross Mountains (Central Poland). Spec. Pap. - Miner. Soc. Pol. 24, 251–255.

Krohe, A., Wawrzenitz, N., 2000. Domainal variations of U–Pb monazite ages and Rb–Sr whole-rock dates in polymetamorphic paragneisses (KTB Drill Core, Germany): influence of strain and deformation mechanisms on isotope systems. J. Metamorph. Geol. 18, 271–291.

Kröner, A., O'Brien, P.J., Nemchin, A.A., Pidgeon, R.T., 2000. Zircon ages for high pressure granulites from South Bohemia, Czech Republic, and their connection to Carboniferous high temperature processes. Contrib. Mineral. Petrol. 138, 127–142.

Kryza, R., 2004. Controversial geochronology: examples from gneisses and granulites of the Góry Sowie (Sudetes, SW Poland). VIII Ogólnopolska Sesja Naukowa "Datowanie minerałów i skał", Kraków, pp. 78–83.

Kukal, Z., 1984. Granitoidové plutony byly hlavním zdrojem živců permokarbonskych sedimentů. Èas. Mineral. Geol. 29 (2), 193–196 (in Czech).

Kusiak, M., Suzuki, K., Paszkowski, M., 2001. Preliminary report of CHIME dating on detrital monazite grains from the Namurian Poruba Beds and the Stephanian Kwaczala Arkose in the Upper Silesia Coal Basin, Poland. J. Earth Planet. Sci., Nagoya Univ. 48, 15–41.

Lekki, J., Lebed, S., Paszkowski, M.L., Kusiak, M., Vogt, J., Hajduk, R., Polak, W., Potempa, A., Stachura, Z., Styczeń, J., 2002. Age determination of monazites using the new experimental chamber of the Cracow proton microprobe. NIMB 210, 472–477.

Mazur, S., Turniak, K., Bröker, M., 2004. Neoproterozoic and Cambro–Ordovician magmatism in the Variscan Kłodzko Metamorphic Complex (West Sudetes, Poland): new insights from U/Pb zircon dating. Int. J. Earth Sci. (Geol. Rundsch.) 93, 758–772.

Montel, J.M., Foret, S., Veschambre, M., Nicollet, Ch., Provost, A., 1996. Electron microprobe dating of monazite. Chem. Geol. 131, 37–53.

Noble, S.R., Searle, M.P., 1995. Age of crustal melting and leucogranite formation from U–Pb zircon and monazite dating in the western Himalaya, Zanskar, India. Geology 23 (12), 1135–1138.

Parrish, R.R., 1990. U–Pb dating of monazite and its application to geological problems. Can. J. Earth Sci. 27, 1431–1450.

Parrish, R.R., Tirrul, R., 1989. U–Pb age of the Baltoro granite, northwest Himalaya, and implications for monazite U–Pb systematics. Geology 17, 1076–1079.

Paszkowski, M., Jachowicz, M., Michalik, M., Teller, L., Uchman, A., Urbanek, Z., 1995. Composition, age and provenance of gravel-sized clasts from the Upper Carboniferous of the Upper Silesia Coal Basin. Stud. Geol. Pol. 108, 45–127.

Paszkowski, M., Kusiak, M., Banaś, M., 1999. New, non-conventional methods in accessory mineral preparation. Documenta Geonica, The 4th Czech-Polish Conference about Carboniferous Sedimentology. Peres Publishers, Prague, pp. 147–150. (in Polish, with English Abstr.)

Petránek, J., 1978. Byly variské plutony Českého masivu tak rychle obnaženy, že se staly zdrojem materialu karbonskych arkóz? Èas. Mineral. Geol. 23 (4), 381–387 (in Czech).

Porębski, S.J., 1981. Świebodzice succession (Upper Devonian–lowest Carboniferous; western Sudetes): a prograding, mass-flow dominated fan-delta complex. Geol. Sudet. 16, 99–190.

Porębski, S.J., 1990. Onset of coarse clastic sedimentation in the Variscan realm of the Sudetes (SW Poland): an example from the Upper Devonian–lower Carboniferous Świebodzice succession. Neues Jahrb. Geol. P-A Abh. 179, 259–274.

Pyle, J.M., Spear, F.S., Wark, D.A., Daniel, C.G., Storm, L.C., 2005. Contributions to precision and accuracy of chemical ages of monazite. Am. Mineral. 90, 547–577.

Rutkowski, J., 1972. Osady stefanu Górnośląskiego Zagłębia Węglowego. Prace IG 61, 539–556 (in Polish, with English Abstr.).

Schandl, E.S., Gorton, M.P., 2004. A textural and geochemical guide to the identification of hydrothermal monazite: criteria for selection of samples for dating epigenetic hydrothermal ore deposits. Econ. Geol. 99, 1027–1035.

Schenck, V., Todt, W., 1981. U–Pb Datierung on Zircon and Monazit der granulite im Moldanubicum Niederosteriechs (Waldviertel). Fortschr. Mineral. 61, 190–191 (in German).

Schneider, D.A., Manecki, M., 2005. Diachronous eclogite and granulite exhumation within the West Sudetes (Bohemia), Poland and Czech Republic. Geophys. Res. Abstr. 7, 04363.

Smellie, J.A.T., Cogger, N., Herrington, J., 1978. Standards for quantitative microprobe determination of uranium and thorium with additional information on the chemical formulae of davidite and euxenite polycrase. Chem. Geol. 22, 1–10.

Suzuki, K., Adachi, M., 1991. The chemical Th–U-total Pb isochron ages of zircon and monazite from the Gray Granite of the Hida terrane, Japan. J. Earth Planet. Sci., Nagoya Univ. 38, 11–37.

Suzuki, K., Adachi, M., 1994. Middle Precambrian detrital monazite and zircon the Hide gneiss on Oki-Dogo Island, Japan: their origin and implications for the correlation of basement gneiss of Southwest Japan and Korea. Tectonophysics 235, 277–292.

Suzuki, K., Adachi, M., 1998. Denudation history of the high T/P Ryoke metamorphic belt, Southwest Japan: constraints from CHIME monazite ages of gneisses and granitoids. J. Metamorph. Geol. 16, 23–37.

Suzuki, K., Adachi, M., Tanaka, T., 1991. Middle Precambrian provenance of Jurassic sandstone in the Mino Terrane, central Japan: Th–U-total Pb evidence from an electron microprobe monazite study. Sediment. Geol. 75, 141–147.

Suzuki, K., Adachi, M., Kajizuka, I., 1994. Electron microprobe observations of Pb diffusion in metamorphosed detrital monazites. Earth Planet. Sci. Lett. 128, 391–405.

Świerczewska, A., 1995. Composition and provenance of Carboniferous sandstones from the Upper Silesia Coal Basin (Poland). Stud. Geol. Pol. 108, 27–43.

Turniak, K., Mazur, S., Wysoczański, R., 2000. SHRIMP zircon geochronology and geochemistry of the Orlica–Śnieżnik gneisses (Variscan belt of Central Europe) and their tectonic implications. Geodin. Acta 13, 293–312.

Van Breemen, O., Aftalion, M., Bowes, O.M., Dudek, A., Misar, Z., Povondra, P., Vrana, S., 1982. Geochronological Studies of the Bohemian Massif, Czechoslovakia, and their significance in the evolution of Central Europe. Trans. R. Soc. Edinb. Earth Sci. 73, 89–108.

Vavra, G., Schaltegger, U., 1999. Post-granulite facies monazite growth and rejuvenation during Permian to Lower Jurassic thermal and fluid events in the Ivrea Zone (Southern Alps). Contrib. Mineral. Petrol. 134, 405–414.

Vlašimský, P., 1986. Příspěvek k diskusi o karbonských arkózách a hloubce denudace variských plutonů. Èas. Mineral. Geol. 31 (4), 429–434.

Williams, M.L., Jercinovic, M.J., Terry, M.P., 1999. Age mapping and dating of monazite on the electron microprobe: deconvoluting multi-stage histories. Geology 27, 1023–1026.

Zhu, X.K., O'Nions, R.K., 1999. Zonation of monazite in metamorphic rocks and its implications for high temperature thermochronology: a case study from the Lewisian terrain. Earth Planet. Sci. Lett. 171 (2), 209–220.

Zulauf, G., Schitter, F., Riegler, G., Finger, F., Fiala, J., Vejnar, Z., 1999. Age constraints on the Cadomian evolution of the Teplá Barrandian unit (Bohemian Massif) through electron microprobe dating of the metamorphic monazite. Z. Dtsch. Geol. Ges. 150/4, 627–639.

Zulauf, G., Bues, C., Dörr, W., Vejnar, Z., 2002. 10 km Minimum throw along the West Bohemian shear zone: evidence for dramatic crustal thickening and high topography in the Bohemian Massif (European Variscides). Int. J. Earth Sci. (Geol. Rundsch.) 91, 850–864.